# **Bearing Spall Size Estimation Under Varying Speed Conditions**

Dang Ngo-The<sup>1</sup>, Cees Taal<sup>2</sup>, and Jérôme Antoni<sup>1</sup>

<sup>1</sup> INSA Lyon, LVA, UR677, 69621 Villeurbanne, France dang.ngo-the@insa-lyon.fr jerome.antoni@insa-lyon.fr

<sup>2</sup> SKF Research and Technology Development (RTD), Houten, the Netherlands cees.taal@skf.com

#### **ABSTRACT**

Accurate estimation of spall size in rolling element bearings is critical for effective diagnostics and prognostics in rotating machinery. Traditional methods often struggle with generalization due to noise and speed variability. This work addresses these limitations by proposing a novel approach that leverages trends in vibration measurements over time and introduces a speed-normalized condition indicator. Building on prior work, we model the bearing fault signal as a periodic pulse wave and derive a Fourier-based representation that links harmonic magnitudes to spall size. We then introduce a normalization technique using harmonic speed ratios to eliminate the influence of the system's transfer function. Experimental validation using controlled lab data confirms the method's ability to preserve signal extrema and improve generalizability over different speeds, offering a promising path toward scalable, real-world bearing health monitoring.

# 1. Introduction

Bearing diagnostics and prognostics using vibration analysis is an important area of research due to its effectiveness in early fault detection and remaining useful life (RUL) estimation of rotating machinery. Vibration signals carry rich information about the dynamic behavior of bearings, enabling the identification of defects such as spalls—localized material losses on the bearing surface.

Bearings have been observed to still operate for a significant amount of time after the appearance of the first spall (Kotzalas & Harris, 2001). Moreover, the propagation of the damage appears to be a rather deterministic process (Rosado, Forster, Thompson, & Cooke, 2009; Mason, Trivedi, & Rosado, 2017). Hence, these properties are promising ingredients to predict the RUL of a spalled bearing, e.g., as was also

Dang Ngo-The et al. This is an open-access article distributed under the terms of the Creative Commons Attribution 3.0 United States License, which permits unrestricted use, distribution, and reproduction in any medium, provided the original author and source are credited.

proposed in (Bolander, Qiu, Eklund, Hindle, & Rosenfeld, 2009).

Unfortunately, estimating the spall size from a vibration signal is not trivial. Typically, existing algorithms try to detect signal characteristics corresponding to the interactions of the rolling element (RE) with the spall, resulting in specific excitations of the system (Epps, 1991; Sawalhi & Randall, 2011; H. Zhang et al., 2021). Although these studies have made important contributions to the understanding of the dynamics of bearing containing systems, the algorithms proposed are difficult to generalize to real applications. The main reason is that these spall-RE interactions might not always be visible due to challenging signal-to-noise ratios not present in clean lab conditions. More recently, a significant amount of pure datadriven methods have also been proposed based on deep learning (S. Zhang, Zhang, Wang, & Habetler, 2020). However, it has been shown that these methods typically lack generalization outside the scope of the trained dataset (Liefstingh, Taal, Restrepo, & Azarfar, 2021) and are difficult to adjust due to their black box nature. Another challenge is that it is not always possible to capture the same type of data on different industrial applications, which demands a feasible method applicable on different setup.

To overcome some of these challenges, it has recently been proposed to investigate multiple vibration measurements over time (i.e., trends) instead of a single vibration measurement (Bublil et al., 2025). Here, it was revealed that for specific setups, detecting extrema over time of bearing fault frequency Fourier magnitudes can be used to estimate the size of large spalls. However, in the work of (Bublil et al., 2025) constant speeds are assumed, while in reality, speed fluctuations will be present. This will distort these signals due to the transfer function, making the detection of extrema challenging. In this work, we propose a new method to eliminate the effect of the transfer function, enabling the use of varying speeds in spall size condition indicators.

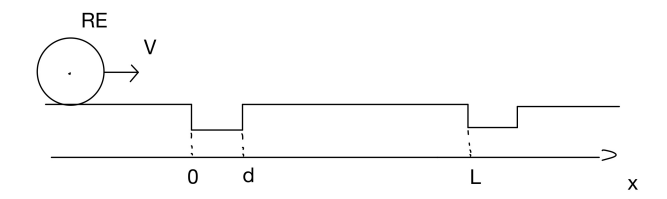


Figure 1. Following the work of (Bublil et al., 2025), the assumption is made that the force signal can be simplified as a pulse wave signal.

### 2. BEARING FAULT MODEL

We first revisit the work of (Bublil et al., 2025) in Figure 1, where the assumption is made that the underlying force signal can be simplified as a pulse wave. Let L denote the distance between two REs, d the spall size and V the RE velocity in circumferential direction. Hence, the spatial distribution of the force, F(x), can be defined with period L as follows,

$$F(x) = F(x+L). (1)$$

Similarly, in the time domain we observe periodicity in T=L/V assuming a constant speed, which gives a force signal f(t)=F(Vt) such that

$$f(t) = f(t+T). (2)$$

Subsequently, by expanding f(t) in its Fourier series as follows,

$$f(t) = \sum_{k \in \mathbb{Z}} f_k e^{j2\pi kt/T}.$$
 (3)

We can use the fact that the Fourier series of a time-domain pulse with varying pulse width can be expressed as a sinc function. Defining  $\tau = Td/L$  as the time the rolling element is over-rolling the spall, we have,

$$f_k = \sin\left(\frac{k\pi\tau}{T}\right)\frac{1}{\pi k} = \sin\left(\frac{k\pi d}{L}\right)\frac{1}{\pi k}.$$
 (4)

It is important to note at this stage that the Fourier coefficients  $f_k$  of the force signal are independent of the speed V and depend only on the geometry of the fault through the ratio d/L. However, this will not be the case for the Fourier coefficients of the acceleration signal.

To facilitate our proposed method in the next section, we introduce the angular frequency  $\Omega=1/T$  which denotes the rotational speed of our machine in Hertz.

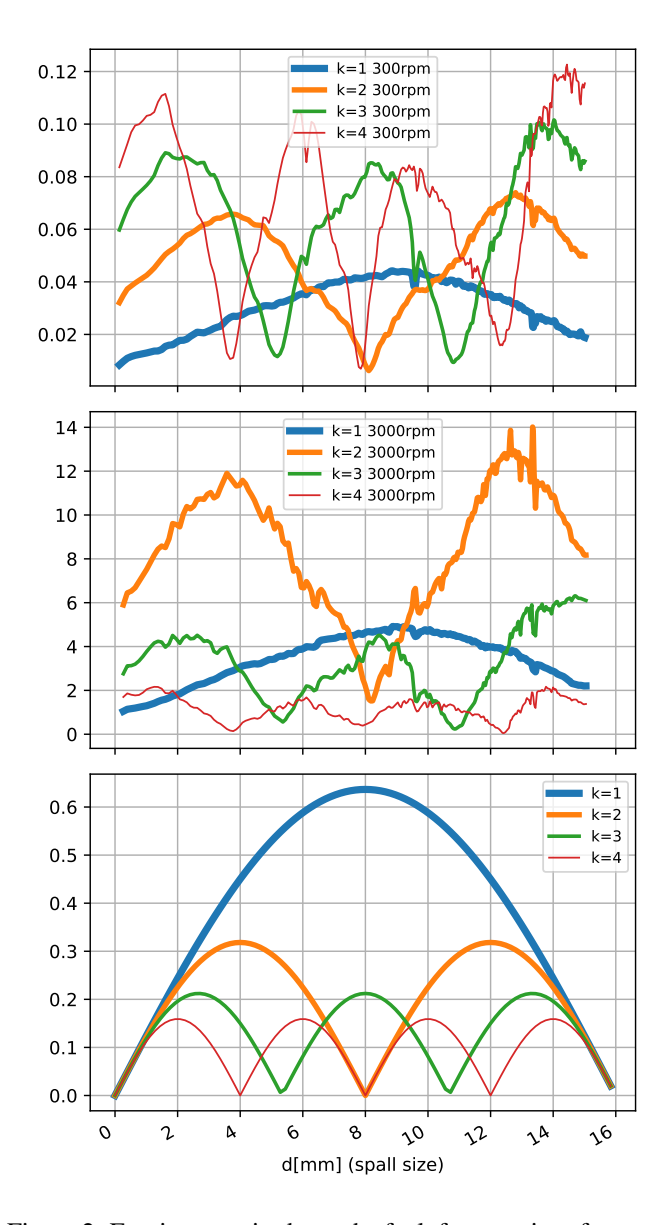


Figure 2. Fourier magnitudes at the fault frequencies of a progressing outer ring spall for speeds 300RPM (top), 3000RPM (middle) and a force model (bottom) with a rolling element distance of 16mm.

Note that in reality, we cannot observe the force signal directly and measure an acceleration signal instead. Therefore,

$$c_k(\Omega) = H(k\Omega) f_k, \tag{5}$$

where  $H(k\Omega)$  stands for the transfer function between force and acceleration at frequency  $k\Omega$ , and  $c_k(\Omega)$  stands for the Fourier coefficient of the acceleration signal with explicit notation of its dependence on speed  $\Omega$ .

An example for the first four harmonics of the aforementioned model is illustrated in the bottom plot of Figure 2 for

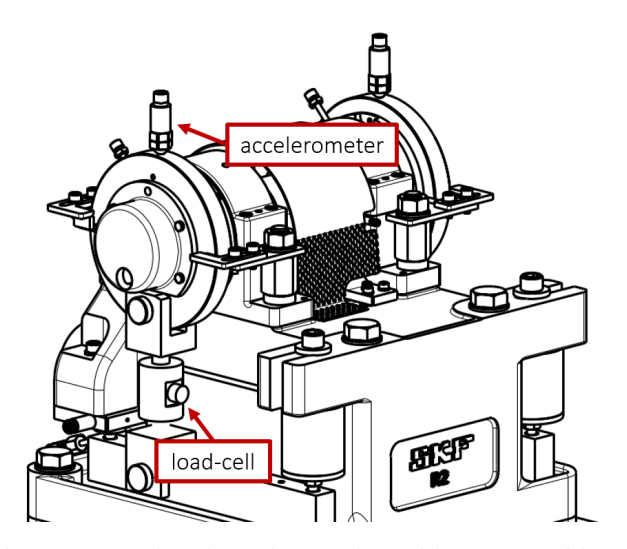


Figure 3. Test-rig schematic overview with sensor positions.

a RE distance of 16 mm where the spall size d progresses from 0 mm to 16 mm. Notice the extrema of the trendlines. For example, a spall size of half of the RE distance results in only the presence of odd harmonics. How to further map this signal to spall sizes the reader is referred to (Bublil et al., 2025).

### 3. SPALL GROWTH EXPERIMENT

To validate our proposed method, we used the experimental data as described in (Bublil, Taal, Maljaars, Klein, & Bortman, 2024). A schematic overview of the test-rig with the sensor placements is shown in Fig.(3). Here, a small outer ring spall is artificially created on an N209 ECP bearing, which is propagated under high load and speed. During intermediate intervals, say after an hour of growth, snapshots of sensor data are recorded for different speeds [300, 332, 500, 600, 750, 1000, 1500 and 3000 rpm]. A lower load is used when recording these snapshots to prevent further spall growth. Hence, for a fixed spall size we obtain a set of vibration recordings for different speeds. The spall size ground truth is based on a load-cell sensor and intermediate visual inspections (see (Bublil et al., 2024) for more details on the load-cell algorithm).

These are used to validate our methods. Moreover, snapshots are recorded at a sample rate of 49152 Hz for a duration of 36 seconds. A tachometer signal with two pulses per shaft rotation is available to accommodate speed fluctuations. This is achieved by means of angular resampling.

A summary of the experimental results is presented in the top two plots in Figure 2. Here, the Fourier magnitude values of the first four harmonics (BPFO) versus the spall size reference is depicted. The top and middle plots represent signals for the frequencies 300 RPM and 3000 RPM, respectively.

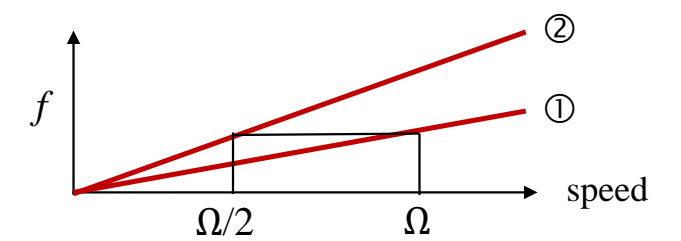


Figure 4. The effect of the transfer function at frequency f is cancelled by dividing the integer-related speed ratios denoted by  $\Omega$ 

Some observations can be made.

- For both speeds, we can clearly see the local maxima and minima of the harmonics aligned with the proposed model from the previous section.
- The harmonic magnitude ratios for a given spall size are not aligned with the model.
- For the two different speeds, the underlying ratios of the harmonics are also different. For example, for 300 RPM we have a dominant fourth harmonic, while the second harmonic is dominant for 3000 RPM.

In the remainder of this paper, we propose a solution for the last two observations. In this manner, we aim to construct a condition indicator for different speeds while preserving the local minima and maxima, as observed for a fixed speed.

# 4. A SPEED NORMALIZED SPALL-SIZE CONDITION INDICATOR

The approach taken is to observe the Campbell diagram. As shown in Figure 4, we observe that the first harmonic order shares the same transfer function as the second harmonic at half its speed denoted by  $\Omega$ . This means that we can ignore the transfer function by calculating the ratio between higher harmonic orders at higher speeds and the first harmonic at lower speeds. By doing so, we can expect to create a plot that has all the minimum points needed for the identification of the spall size without the necessity of estimating the transfer function, which is not always feasible. Based on the relationship (5), one has

$$c_k\left(\frac{\Omega}{k}\right) = H\left(\Omega\right)f_k,$$
 (6)

so that the ratio

$$\frac{c_k(\frac{\Omega}{k})}{c_1(\Omega)} = \frac{f_k}{f_1} \tag{7}$$

is found independent of H(f). For example, taking k=2,

$$c_2\left(\frac{\Omega}{2}\right) = H\left(\Omega\right)f_2,\tag{8}$$

and

$$\frac{c_2\left(\frac{\Omega}{2}\right)}{c_1(\Omega)} = \frac{f_2}{f_1}.\tag{9}$$

Using the recorded speeds, this produces the following invariants<sup>1</sup>:

$$\frac{c_2 (1500)}{c_1 (3000)} = \frac{c_2 (750)}{c_1 (1500)} = \frac{c_2 (500)}{c_1 (1000)}$$

$$= \frac{c_2 (375)}{c_1 (750)} = \frac{c_2 (300)}{c_1 (600)}.$$
(10)

It is beneficial to inspect the trend lines of the first four harmonics to better estimate the spall size, since the fourth harmonic trend line divides the spall size range into 4 equal parts, as shown in Figure 2. The first harmonic is chosen as the denominator since its trend line hold a singular parabolic shape, it allows the ratio to retain the location of the minima. These points contribute to the ability to estimate the spall size by comparing with experimental results.

## 5. RESULTS

The results of the proposed method based on the Fourier magnitude ratios to eliminate the effect of the transfer function are shown in Figure 5. The top figure shows harmonic ratio 2, the center plot harmonic ratio 3 and the bottom plot harmonic ratio 4. The dashed line in each plot shows the results of the force model. For example, following Equation 4, the top figure illustrates  $c_2/c_1$  with L=16 with varying spall size d on the x-axis.

Within each speed ratio, we can clearly observe a highly consistent transfer function normalization, regardless of the specific speeds selected. Moreover, the signal minima and maxima are perfectly preserved, even for different speeds, in contrast to what was shown in Figure 2. Consequently, we can map these extrema of the signal to spall sizes as proposed in (Bublil et al., 2025), while also considering different speeds, provided that they are defined in harmonic ratios.

From the figure, we also observe that the overall condition indicator values tend to be lower than those predicted by the proposed model. This bias tends to be larger for higher harmonic ratios. One possible reason could be that the underlying force model does not follow a perfect pulse wave, but perhaps a more smooth waveform resulting in a faster drop of harmonic amplitudes. More research is needed to validate this.

# 6. DISCUSSION AND CONCLUSIONS

This study proposes a new bearing spall-size condition indicator under varying operating speeds using harmonic speed

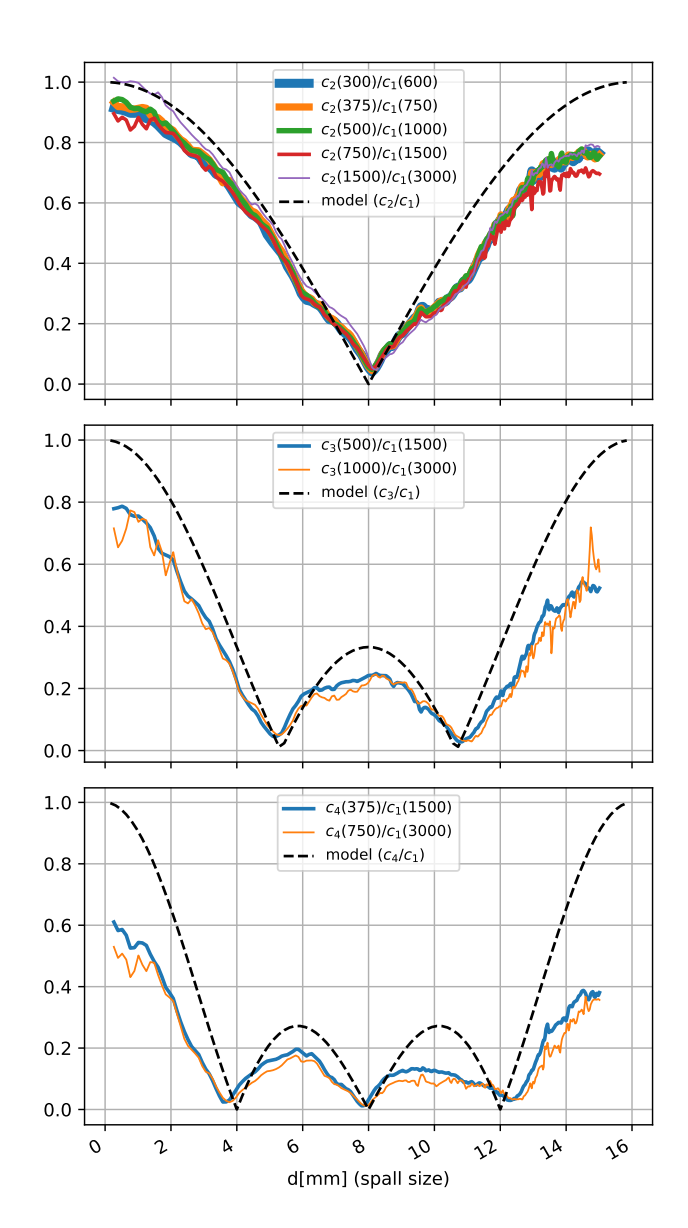


Figure 5. Fourier magnitude ratios at the outer ring harmonic fault frequencies of a progressing outer ring spall for speed ratios 2 (top), 3 (center) and 4 (bottom). Dashed line shows analytical signals based on the force model.

ratios in vibration signals. By eliminating the influence of the system transfer function, the proposed approach enables consistent signal extrema across different speeds, significantly enhancing the reliability and scalability of spall size estimation. Experimental validation confirms the effectiveness of the method, laying the groundwork for more accurate and generalizable health indicators in real-world bearing diagnostics and prognostics.

The force model used in this work represents approximately the response that we could expect from a rectangular spall. However, the reality shows that there is a difference in am-

 $<sup>^1</sup>$  Note that  $\Omega$  is in Hz, but for reasons of interpretation we write the argument of  $c_k(.)$  in RPM

plitude of pulse signal at entry and exit of the spall. Further research is required to further validate the generalizability of the proposed model beyond the current test rig setup. It is also important to note that in real applications, spalls hold different shapes, which might alter the excitation signal. Therefore, it could be interesting to investigate the effect of different force models on the method proposed by this work.

A further limitation of the proposed method is its reliance on vibration data at two speeds in a harmonic (integer) ratio, such as 300/600 RPM. This makes it most suitable for variable-speed applications with discrete speed steps. An example is the pulp and paper industry, where gradual ramp-up protocols are used to prevent thermal stress, although similar practices exist in other sectors as well.

### REFERENCES

- Bolander, N., Qiu, H., Eklund, N., Hindle, E., & Rosenfeld, T. (2009). Physics-based remaining useful life prediction for aircraft engine bearing prognosis. In *Annual conference of the phm society* (Vol. 1).
- Bublil, T., Taal, C., Maljaars, B., Klein, R., & Bortman, J. (2024). Labeling algorithm for outer-race faults in bearings based on load signal. In *Phm society european conference* (Vol. 8, pp. 7–7).
- Bublil, T., Taal, C., Maljaars, B., Matania, O., Klein, R., & Bortman, J. (2025). Experimental study on condition indicators for severity estimation of growing spalls in bearings. *Mechanical Systems and Signal Processing*, 236, 113019.
- Epps, I. K. (1991). An investigation into vibrations excited by discrete faults in rolling element bearings. University of Canterbury. Mechanical Engineering.
- Kotzalas, M. N., & Harris, T. A. (2001). Fatigue failure progression in ball bearings. *J. Trib.*, 123(2), 238–242.
- Liefstingh, M., Taal, C., Restrepo, S. E., & Azarfar, A. (2021). Interpretation of deep learning models in bearing fault diagnosis. In *Annual conference of the phm society* (Vol. 13).
- Mason, J. K., Trivedi, H. K., & Rosado, L. (2017). Spall propagation characteristics of refurbished vim–var aisi m50 angular contact bearings. *Journal of Failure Analysis and Prevention*, 17(3), 426–439.
- Rosado, L., Forster, N. H., Thompson, K. L., & Cooke, J. W. (2009). Rolling contact fatigue life and spall propagation of aisi m50, m50nil, and aisi 52100, part i: Experimental results. *Tribology Transactions*, 53(1), 29-41.
- Sawalhi, N., & Randall, R. (2011). Vibration response of spalled rolling element bearings: Observations, simulations and signal processing techniques to track the

- spall size. *Mechanical Systems and Signal Processing*, 25(3), 846–870.
- Zhang, H., Borghesani, P., Smith, W. A., Randall, R. B., Shahriar, M. R., & Peng, Z. (2021). Tracking the natural evolution of bearing spall size using cyclic natural frequency perturbations in vibration signals. *Mechanical Systems and Signal Processing*, 151, 107376.
- Zhang, S., Zhang, S., Wang, B., & Habetler, T. G. (2020). Deep learning algorithms for bearing fault diagnostics—a comprehensive review. *IEEE Access*, 8, 29857-29881.

## **BIOGRAPHIES**



Dang Ngo The (M.S in Mechanical Engineering, 2025) is a doctoral student in the field of dynamic behavior of gears and bearings. Graduated from Institut National des Sciences Appliquées de Lyon (INSA de Lyon), he is currently working at Laboratoire de Mécaniques des Contacts et des Structures (LaMCoS).



Cees Taal is an experienced researcher in the field of sensor signal processing and machine learning. He has worked in academia—at Delft University of Technology (Delft, The Netherlands) and KTH Royal Institute of Technology (Stockholm, Sweden)—on audio and speech processing. Following his academic career, he held var-

ious industrial positions in biomedical engineering at Philips Research (Eindhoven, The Netherlands) and in the energy sector at Eneco (Rotterdam, The Netherlands). He is currently appointed as a Senior Technologist at SKF, The Netherlands, where he is responsible for defining the research strategy in the field of bearing diagnostics and prognostics. Cees received the IEEE Signal Processing Society Best Paper Award in 2016.



Jerome Antoni (M.S. in Mechanical Engineering, 1995, Ph.D. in Signal Processing, 2000, University of Technology of Compiègne) joined the University of Technology of Compiègne in 2001, after completing his PhD at the University of Grenoble (France). He currently holds a full professor position at INSA Lyon, University of

Lyon, France, and leads the research group Laboratoire Vibrations Acoustique. The main direction of his research activity is concerned with the development of signal processing methods in mechanical applications, with a particular interest in the resolution of inverse problems in acoustics and vibrations. This includes applications in machine and structural health monitoring, identification and imaging of acoustic and vibration sources. He has published more than two hundred journal papers in these domains. Jerome Antoni is Associate Editor of Mechanical Systems and Signal Processing and with the editorial boards of Applied Sciences and Machines.